TAK1 is an Essential Regulator of BMP Signalling in Cartilage

Citation

Shim, Jae-Hyuck, Matthew B. Greenblatt, Min Xie, Michael D. Schneider, Weiguo Zou, Bo Zhai, Steven Gygi, and Laurie H. Glimcher. 2009. TAK1 is an essential regulator of BMP signalling in cartilage. The EMBO Journal 28(14): 2028-2041.

Published Version

doi:10.1038/emboj.2009.162

Permanent link

http://nrs.harvard.edu/urn-3:HUL.InstRepos:4891679

Terms of Use

Share Your Story

The Harvard community has made this article openly available.
Please share how this access benefits you. Submit a story .

Accessibility

TAK1 is an essential regulator of BMP signalling in cartilage

Jae-Hyuck Shim[1,6], Matthew B Greenblatt[1,6], Min Xie[2], Michael D Schneider[3], Weiguo Zou[1], Bo Zhai[4], Steven Gygi[4] and Laurie H Glimcher*[,1,5]

[1]Department of Immunology and Infectious Diseases, Harvard School of Public Health, Boston, MA, USA, [2]Department of Internal Medicine, University of Texas Southwestern Medical Center, Dallas, TX, USA, [3]National Heart and Lung Institute, Imperial College London, London, UK, [4]Department of Cell Biology, Harvard Medical School, Boston, MA, USA and [5]Department of Medicine, Harvard Medical School, Boston, MA, USA

TGFβ activated kinase 1 (TAK1), a member of the MAPKKK family, controls diverse functions ranging from innate and adaptive immune system activation to vascular development and apoptosis. To analyse the *in vivo* function of TAK1 in cartilage, we generated mice with a conditional deletion of *Tak1* driven by the collagen 2 promoter. *Tak1*col2 mice displayed severe chondrodysplasia with runting, impaired formation of secondary centres of ossification, and joint abnormalities including elbow dislocation and tarsal fusion. This phenotype resembled that of bone morphogenetic protein receptor (BMPR)1 and *Gdf5*-deficient mice. BMPR signalling was markedly impaired in TAK1-deficient chondrocytes as evidenced by reduced expression of known BMP target genes as well as reduced phosphorylation of Smad1/5/8 and p38/Jnk/Erk MAP kinases. TAK1 mediates Smad1 phosphorylation at C-terminal serine residues. These findings provide the first *in vivo* evidence in a mammalian system that TAK1 is required for BMP signalling and functions as an upstream activating kinase for Smad1/5/8 in addition to its known role in regulating MAP kinase pathways. Our experiments reveal an essential role for TAK1 in the morphogenesis, growth, and maintenance of cartilage.

*Corresponding author. Department of Immunology and Infectious Diseases, Harvard School of Public Health, Infectious Diseases, Building FXB, Room 205, 651 Huntington Avenue, Boston, MA 02115, USA. Tel.: +1 617 432 0622; Fax: +1 617 432 0084; E-mail: lglimche@hsph.harvard.edu
[6]These authors contributed equally to this work

Introduction

During endochondral ossification, mesenchymal stem cells undergo a highly organized differentiation program during which they condense and differentiate into chondrocytes, forming the template for bone formation (Kronenberg, 2003; Yoon and Lyons, 2004). Bone morphogenic proteins (BMPs) were originally isolated as proteins that promote ectopic cartilage and bone formation (Wozney *et al*, 1988). Further studies have confirmed the role of BMPs in cell proliferation, differentiation, and apoptosis during cartilage and bone formation and revealed additional functions in other developmental processes (Yoon and Lyons, 2004). For example, BMP-2 and BMP-4 are essential for the induction of ventral mesoderm formation during early mouse development (Winnier *et al*, 1995). BMP family members transduce signals through heteromeric complexes of type II and type I transmembrane serine/threoine kinase receptors. Type II receptor ligation initiates the recruitment of type I receptors to form heteromeric receptor complexes that are then trans-phosphorylated. The type I receptors in turn initiate Smad signalling by phosphorylating the receptor-regulated Smads, R-Smad1/5/8. Once phosphorylated, R-Smads associate with Smad4 and accumulate in the nucleus to regulate gene expression (Massague, 1998). In addition to the Smad-dependent pathway, BMPs can also activate TGFβ activated kinase 1 (TAK1) leading to MKK3/6-mediated p38 MAP kinase activation. However, the mechanism by which TAK1 regulates BMP signalling in chondrocytes is largely unknown (Derynck and Zhang, 2003).

TAK1, a member of the MAPKKK family, was originally identified as a key regulator of MAPK kinase activation in TGFβ and BMP signalling pathways (Yamaguchi *et al*, 1995). In *Xenopus* development, TAK1 mediates mesoderm induction and patterning downstream of BMP ligands (Shibuya *et al*, 1998). Mutations in the mouse *Tak1* gene causes defects in the developing intraembryoinc vasculature and yolk sac, phenotypes similar to those caused by loss of function mutations in SMAD5 (Chang *et al*, 1999; Shim *et al*, 2005; Jadrich *et al*, 2006), suggesting that TAK1 may be important for Smad activation downstream of BMP stimulation. However, no biochemical or *in vivo* functional data currently exist to support this hypothesis.

Because of the early lethality of mice with a germline deletion of *Tak1*, cellular studies in these mice were limited to mouse embryonic fibroblasts (MEFs). TAK1-deficient MEFs displayed normal activation of canonical Smads after TGFβ stimulation, despite displaying a block in NF-κB and JNK activation by microbial products in the innate immune system (Shim *et al*, 2005). TAK1 also has critical functions in the regulation of adaptive immunity where it is required for antigen receptor signalling in both T cells and B cells through

its regulation of NF-κB and JNK activation (Sato *et al*, 2005, 2006; Liu *et al*, 2006; Wan *et al*, 2006). In addition to its role in the immune system, TAK1 functions as a key regulator of vascular development and keratinocyte proliferation, differentiation, and apoptosis (Omori *et al*, 2006; Sayama *et al*, 2006) and mediates survival of hematopoietic cells and hepatocytes through its regulation of NF-κB and JNK activation (Tang *et al*, 2008).

Given earlier studies suggesting a role for TAK1 in signalling downstream of both the BMP and TGFβ signalling pathways and the importance of these pathways for chondrocyte biology, we decided to generate mice with cartilage-specific deletion of the *Tak1* gene to address the physiological roles of mammalian TAK1 in cartilage. Deletion of *Tak1* in chondrocytes resulted in a dramatic runting phenotype with chondrodysplasia and joint abnormalities similar to that seen in mice deficient in BMP signalling. Biochemical analysis of TAK1-deficient chondrocytes confirmed a defect in BMP signalling that unexpectedly resulted in impaired Smad1/5/8 activation in addition to defective p38/Jnk/Erk MAP kinase signalling. We provide the first evidence that TAK1 is required for the normal development and preservation of cartilage.

Results

Expression of TAK1 in cartilage

As the expression pattern for TAK1 in cartilage is unknown, we stained for TAK1 using immunohistochemistry (IHC) on coronal tibial sections from a postnatal day 20 (p20) mouse (Figure 1). TAK1 staining was largely restricted to prehypertrophic and hypertrophic chondrocytes. Hypertrophic chondrocytes from both the terminal growth plate and the area surrounding the secondary centre of ossification showed positive staining. Additionally, TAK1 expression in E16.5 embryos was examined. TAK1 is widely expressed in multiple embryonic cartilage tissues, including the chondroepiphyses of the long bones, the laryngeal and tracheal cartilage, and the developing frontal bone (Supplementary Figure S1).

Abnormal cartilage development in TAK1-deficient mice

To determine the role of TAK1 in cartilage development, we generated mice lacking *Tak1* in cartilage by intercrossing a *Tak1* floxed-allele strain of mice with a type II collagen-cre deleter strain (Ovchinnikov *et al*, 2000). IHC for TAK1 expression confirmed deletion specifically in chondrocytes, with staining absent in both the terminal growth plate and the hypertrophic chondrocytes surrounding the secondary centre of ossification (Figure 1). Animals homozygous for the floxed allele expressing the cre transgene (hereafter referred to as *Tak1*[col2] mice) displayed severe postnatal growth retardation culminating in death by 2–3 weeks of age (Figure 2A). As shown in Alizarin red S/Alcian blue stained skeletal preps of p20 mice, *Tak1*[col2] mice showed proportional shortening of the long bones of the limbs, a 'doming' of the cranium, malocclusion, and kyphosis of the thoracic spine (Figure 2A). *Tak1*[col2] postnatal day 0 (p0) offspring showed a modest reduction in the length of long bones and disorganization of proliferating chondrocyte columns in the growth plate (Supplementary Figure S2A and B). Animals heterozygous for the floxed allele expressing the cre transgene showed no appreciable phenotype at any age (data not shown). Histologic analysis of coronal sections of
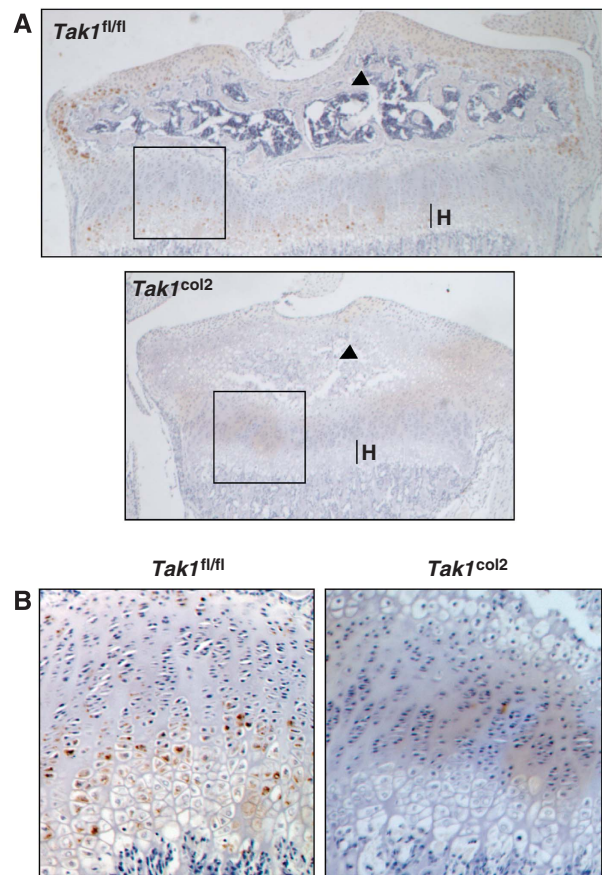

Figure 1 Expression of TAK1 in the proximal tibia. (**A**) Immunohistochemistry for TAK1 showing expression in a coronal section of the proximal tibias of *Tak1*^{fl/fl} and *Tak1*[col2] mice. Secondary centres of ossification are indicated with arrows, hypertrophic chondrocytes in the terminal growth plate are indicated with an 'H'. (**B**) High power of the indicated areas of (A), showing TAK1 expression in prehypertrophic and hypertrophic chondrocytes.

Tak1[col2] tibias confirmed a marked reduction in overall size (Figure 2B). Additionally, the formation of secondary ossification centres was delayed, with *Tak1*[col2] mice showing only minimal vascular invasion and calcification within the secondary centre of ossification. Notably, *Tak1*[col2] chondrocytes surrounding the secondary ossification centre progressed normally through the hypertrophic stage of differentiation (Figure 2B, arrow).

To determine whether the runting observed in *Tak1*[col2] mice is the result of a delay in endochondral ossification of long bones, we performed *in situ* hybridization for osteopontin on femurs from E16.5 embryos to highlight the ossified portion of the bone (Supplementary Figure S2C). As *Tak1*[col2] embryos displayed a similar extent of ossification, it is unlikely that the runting phenotype observed postnatally is the result of defects in the early stages of endochondral ossification. The long bones of E18.5 embryos were similarly of comparable length to wild-type controls (data not shown). Finally, *in situ* hybridization of Collagen Xα (ColX) was performed to determine the effects of TAK1 deletion on chondrocyte maturation (Figure 2C). Although p20 mice displayed a moderate reduction in the size of the prehypertrophic/hypertrophic zone of ColX-positive chondrocytes, E16.5 and E18.5 embryos were found to display normal
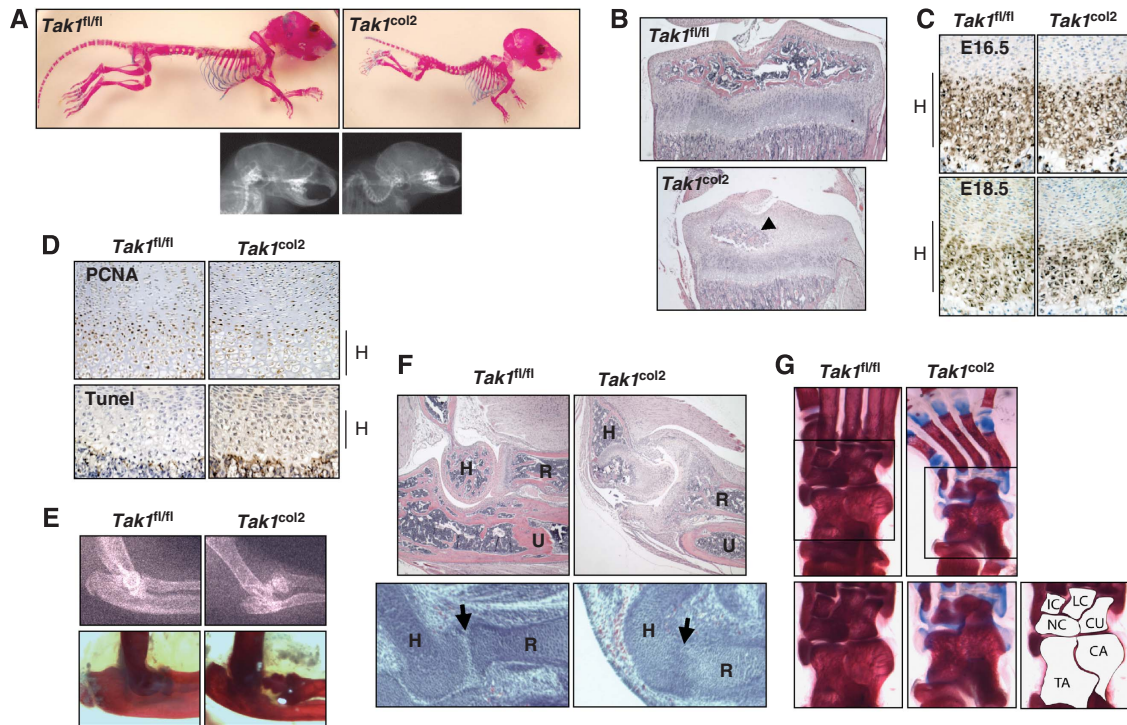
Figure 2 Abnormal cartilage development of TAK1-deficient mice. (**A**) Skeletal preparations of 3 week old $Tak1^{fl/fl}$ and $Tak1^{col2}$ mice (upper panels). X-ray of the skull of 3 week old $Tak1^{fl/fl}$ and $Tak1^{col2}$ mice, showing doming of the skull and malocclusion in $Tak1^{col2}$ mice (lower panels). (**B**) Histological analysis of the proximal tibia of $Tak1^{fl/fl}$ and $Tak1^{col2}$ mice. Haematoxylin and eosin-stained sections through the proximal tibia of 3 week old $Tak1^{fl/fl}$ and $Tak1^{col2}$ mice. The proximal tibia of $Tak1^{col2}$ mice is smaller and shows impaired formation of secondary ossification centres (indicated with an arrow). (**C**) *In situ* hybridization for Collagen X (ColX) in the proximal humerus of E16.5 and E18.5 $Tak1^{fl/fl}$ and $Tak1^{col2}$ mice, demonstrating similar extent of chondrocyte hypertrophy. (**D**) PCNA (top panel) and TUNEL (bottom panel) staining on the chondroepiphyses of p0 $Tak1^{fl/fl}$ and $Tak1^{col2}$ mice, demonstrating a decrease in PCNA-positive cells and an increase in TUNEL-positive terminal hypertrophic chondrocytes. (**E**) X-rays and alizarin red/alcian blue stained skeletal preparations of the elbows of 3 week old $Tak1^{fl/fl}$ and $Tak1^{col2}$ mice, showing dislocation in $Tak1^{col2}$ mice. (**F**) Histological analysis of the elbow of $Tak1^{fl/fl}$ and $Tak1^{col2}$ mice. Haematoxylin and eosin-stained sections through elbows of p20 and E14.5 $Tak1^{fl/fl}$ and $Tak1^{col2}$ mice. $Tak1^{col2}$ mice show an overgrowth of the cartilage on the distal humerus and a widening of the proximal radius. The humerus (H), radius (R), and ulna (U) are labelled. (**G**) High-power view of the ankle of alizarin red/alcian blue stained skeletal preparations of 3 week old $Tak1^{fl/fl}$ and $Tak1^{col2}$ mice, showing fusion of the tarsal bones and medial dislocation of the phalanges. C, intermediate cuneiform; LC, lateral cuneiform; CU, cuboid; NC, navicular; CA, calcaneus; TA, talus.

growth plate architecture. Taken together, these data indicate that the runting phenotype observed in $Tak1^{col2}$ mice has an onset sometime between E18.5 and birth.

The overall reduction in the size of the $Tak1^{col2}$ chondroepiphysis could be due to increased chondrocyte apoptosis or decreased chondrocyte proliferation. To determine the relative contributions of each, $Tak1^{col2}$ chondroepiphyses were stained for proliferating cell nuclear antigen (PCNA) as an index of cell proliferation and by terminal deoxynucleotidyl transferase dUTP nick end labelling (TUNEL) as a marker for apoptotic cells (Figure 2D). $Tak1^{col2}$ chondroepiphyses displayed both a decrease in chondrocyte proliferation in the prehypertrophic/proliferating zone of the growth plate and an increase in the apoptosis of terminal hypertrophic chondrocytes, indicating that both mechanisms contribute to the decrease in the size of the chondroepiphysis.

Radiographs revealed dislocation of the elbow and a corresponding lateral deviation of the forearm in $Tak1^{col2}$ mice (Figure 2E, upper panels). The penetrance of this phenotype was ~80% by two weeks of age. Alizarin red/ alcian blue stained skeletal preparations of the elbow showed a similar disruption of the elbow architecture with the formation of ectopic calcifications in the joint space

(Figure 2E, lower panels). Tissue sections taken parallel to the long axis of the forelimb showed that this phenotype corresponds with an overgrowth of the articular cartilage on the distal humerus facing the radius (Figure 2F, upper panels). The proximal end of the radius has expanded extensively around the protruding articular cartilage of the humerus to the point of displacing the normal articulation between the ulna and the distal humerus. To determine whether the elbow phenotype observed postnatally represents a developmental defect in joint formation, we examined the elbow joint of E14.5 embryos (Figure 2F, lower panels). The distal humerus and the proximal radius were present as a single continuous skeletal element in $Tak1^{col2}$ embryos, whereas control embryos showed a clear cavitation of the joint and a separation of the two skeletal elements. Cavitation of the joint between the humerus and the ulna occurred normally (data not shown). Considering that histologic analysis of the p20 elbow joint shows the presence of a joint space between the distal humerus and proximal radius, this indicates that $Tak1^{col2}$ mice display a delay in cavitation of the humero-radial joint space.

In addition, as shown in the high-power views of skeletal preparations (Figure 2G), the phalanges of the hindlimbs show a marked medial deviation and the tarsals show a

failure to separate during development, the cuboid, lateral cuneiform, intermediate cuneiform, navicular, and calcaneus all forming a continuous skeletal element. Although the tarsals of the littermate control mouse show complete ossification by 20 days of age, the fused tarsal element of $Tak1^{col2}$ mice shows incomplete ossification with a layer of Alcian blue positive cartilage surrounding the ossified centre. In contrast, the hip, shoulder, and temperomandibular joints showed no signs of developmental abnormalities (data not shown). Thus, $Tak1^{col2}$ mice show both impaired growth of skeletal elements and defects in the elbow and tarsal joints. In this respect, they resemble a mixture of the tarsal and elbow abnormalities observed in GDF5-deficient mice and the long bone abnormalities present in mice lacking BMP 2/4/7 (Storm *et al*, 1994).

Reduced levels of BMP signalling in TAK1-deficient mice

Overall phenotypic similarities between $Tak1^{col2}$ mice and mice with specific deletions of multiple BMP receptor subunits in chondrocytes suggested a role for TAK1 in BMP signalling pathways (Yoon *et al*, 2005). To address this possibility directly, we performed immunostaining analysis for the phosphorylation of Smad 1/5/8 (BMP-responsive Smads) in the proximal tibia of $Tak1^{fl/fl}$ and $Tak1^{col2}$ mice. Phosphorylation levels of Smad1/5/8 were significantly reduced in the hypertrophic chondrocytes of $Tak1^{col2}$ mice

(Figure 3A). Similarly, immunoblotting analysis of primary chondrocytes showed decreased basal levels of phosphorylated Smad 1/5/8 in TAK1-deficent chondrocytes derived from p0 $Tak1^{col2}$ mice, as compared with littermate control chondrocytes (Figure 3B). However, $Tak1$ deletion did not affect the *ex vivo* basal phosphorylation levels of Smad2, and levels of Smad1 and Bmpr1A protein in TAK1-deficient chondrocytes were comparable to wt chondrocytes (Figure 3B). Hence, $Tak1$ deletion results in reduced levels of activated Smad1/5/8 *in vivo* implying that TAK1 may regulate BMP-responsive Smad activation (Smad1/5/8), but not TGFβ-responsive Smad activation (Smad2). In addition, TAK1 appears to regulate Smad phosphorylation rather than altering expression of BMP signalling components. P38 is also known to be phosphorylated downstream of BMP stimulation; however, we were unable to determine phospho-p38 levels in cartilage *in vivo* by IHC, despite multiple attempts.

As BMP signalling was reduced in both *in vivo* and *ex vivo* measurements of phosphorylated signalling intermediates in $Tak1^{col2}$ mice, we examined expression levels of known BMP target genes *in vivo*. Indian hedgehog (IHH) is a key regulator of bone formation that coordinates both chondrocyte proliferation/differentiation and osteoblast differentiation (Kronenberg, 2003). Mice in which chondrocytes are genetically unable to respond to BMPs show decreased expression of IHH in prehypertrophic chondrocytes, and this is proposed
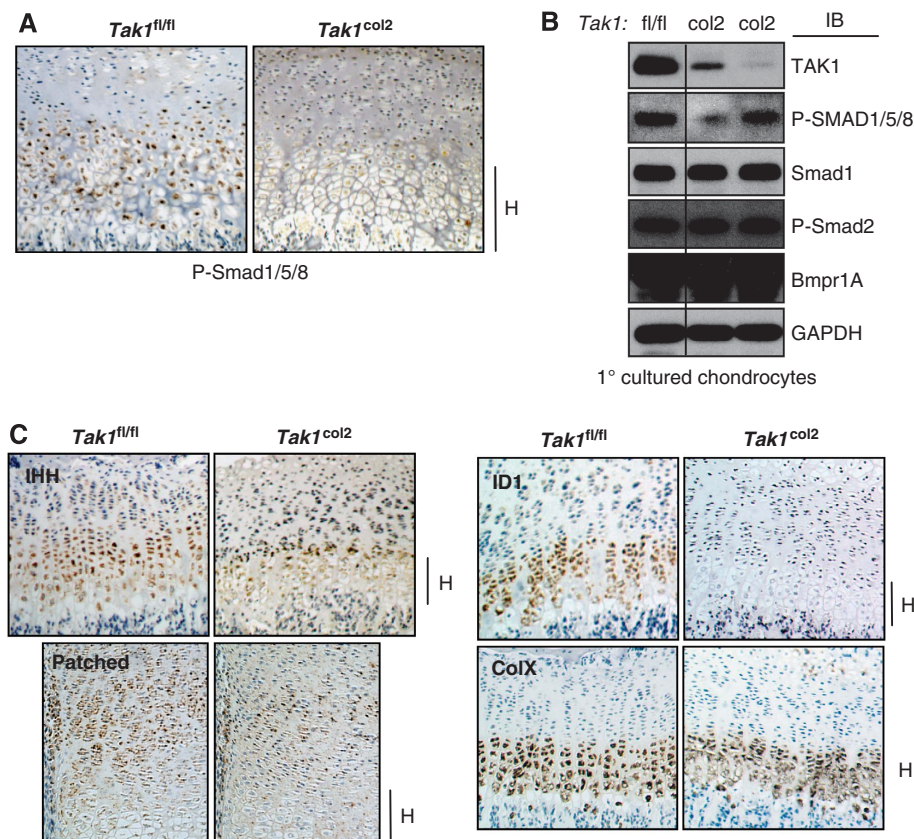

Figure 3 Reduced BMP signalling in TAK1-deficient mice. (**A**) Immunohistochemistry for phosphorylation of BMP-responsive Smad proteins. Coronal sections of the proximal tibia of P0 $Tak1^{fl/fl}$ and $Tak1^{col2}$ pups were stained with anti-phospho-Smad1/5/8 antibody. Hypertrophic chondrocytes in the terminal growth plate are indicated with an 'H'. (**B**) Primary chondrocytes were isolated from cartilage tissues of p0 $Tak1^{fl/fl}$ and $Tak1^{col2}$ mice, cultured for 3 days, and immunoblotted with the indicated antibodies. (**C**) *In situ* hybridization for IHH, Patched, ID1, and Collagen Xα (ColX). Coronal sections of the proximal tibia of 3 week old $Tak1^{fl/fl}$ and $Tak1^{col2}$ mice were probed for the expression of the indicated mRNAs. The hypertrophic region of the growth plate is shown.

as a major contributor to the limb growth retardation seen in these mice (Grimsrud *et al*, 2001; Yoon *et al*, 2006). We tested whether a similar reduction in IHH might contribute to the runting seen in *Tak1*^col2 mice (Figure 3C, left panels). *In situ* hybridization of the proximal tibia with IHH probes showed a moderate decrease of IHH transcript levels in the hypertropic chondrocytes of *Tak1*^col2 mice. To show that this reduction in IHH transcript levels resulted in a functional decrease in IHH signalling *in vivo*, we also performed *in situ* hybridization to quantify levels of the IHH target gene, patched (Figure 3C, left panels). Patched expression was reduced in both prehypertrophic chondrocytes and in the bone collar. The reduction in patched expression even outside of cartilage strongly suggests that TAK1 functions upstream of IHH expression in hypertrophic chondrocytes and not in signal transduction downstream of IHH.

To confirm a functional defect in BMP signalling *in vivo*, we performed *in situ* hybridization to measure the transcript levels of *Id1*, a known BMP target gene in multiple systems (Miyazono and Miyazawa, 2002). ID1 expression was almost completely ablated in the hypertrophic chondrocytes of *Tak1*^col2 mice, whereas expression of type X collagen (ColX), the major extracelluar matrix marker for hypertrophic chondrocytes, was little affected by *Tak1* deletion, showing only a modest reduction in the overall size of the hypertrophic zone (Figure 3C, right panels). These findings suggest that TAK1 is indispensable for the *in vivo* response to BMPs in the terminal growth plate.

Impaired BMP signalling in TAK1-deficient chondrocytes

BMP signalling through Smad1/5/8 is required for the induction of several canonical BMP target genes, including *Id1*, *Msx1*, and *Noggin* (Kameda *et al*, 1999; Miyazono and Miyazawa, 2002; Wan and Cao, 2005; Binato *et al*, 2006). We analysed the induction of these BMP target genes in primary TAK1-deficient chondrocytes by using a quantitative RT–PCR assay (Figure 4A). After activation by BMP2/7, wt but not TAK1-deficient chondrocytes showed an appreciable induction in levels of Id1, Msx1, and Noggin transcripts consistent with a role for TAK1 in mediating BMP-induced gene expression in chondrocytes.

To facilitate further biochemical analysis, we immortalized primary chondrocytes derived from *Tak1*^fl/fl and *Tak1*^col2 newborn offspring by stably transfecting them with the SV40 large T antigen (Kobayashi *et al*, 2005; Shim *et al*, 2005). Immunoblotting for TAK1 confirmed a significant reduction in TAK1 expression in *Tak1*^col2 relative to *Tak1*^fl/fl chondrocytes (Supplementary Figure S3A). As deletion of *Tak1* by col2-cre is not 100% efficient and chondrocytes were maintained as bulk cultures rather than colonies to avoid clonal artifacts, residual TAK1 expression is present in *Tak1*^col2 chondrocyte cultures. We tested the requirement for TAK1 in BMP or TGFβ signalling by measuring BMP/TGFβ-dependent promoter activation. Cells were transfected with BMP or TGFβ-responsive luciferase reporters and stimulated with BMP2/7 or TGFβ (Figure 4B and C). *Tak1*^fl/fl chondrocytes showed approximately two-fold induction in luciferase reporter activity in response to BMP2/7, whereas *Tak1*^col2 chondrocytes showed no response. Similarly, overexpression of a catalytically inactive TAK1 mutant (ΔN/K63W; hereafter CI) blocked gene induction in wt chondrocytes in response to

BMP2/7 (Figure 4B, right panel). TGFβ-induced luciferase reporter activity was not affected by *Tak1* deletion, suggesting that, in chondrocytes, TAK1 is important for BMP but not TGFβ signalling (Figure 4C).

Reduced activation of Smad and MAP kinase pathways by BMPs in TAK1-deficient chondrocytes

It has been reported that BMP signalling is mediated by two distinct pathways: the canonical Smad pathway and the TAK1-p38 MAP kinase pathway (Derynck and Zhang, 2003). We examined the activation of these two arms of BMP signalling in TAK1-deficient chondrocytes by immunoblotting with antibodies specific for phospho-Smad1/5/8 and phospho-p38 (Figure 4D). In the absence of TAK1, Smad1/5/8 phosphorylation was moderately decreased, and a small, but reproducible decrease in the electrophoretic mobility of phosphorylated Smad proteins was detected. However, *Tak1* deletion did not affect total Smad1 protein levels, implying that TAK1 regulates Smad phosphorylation rather than altering expression of Smad1/5/8 (Supplementary Figure S3C). *Tak1*^col2 chondrocytes exhibited impaired activation of p38, Erk1/2, and Jnk1/2 MAP kinases in response to BMP2/7, implying that TAK1 may function as a key regulator of BMP-mediated MAP kinase activation (Figure 4D and E). Immunofluorescence staining for phospho-Smad1/5/8 after BMP2/7 stimulation showed that phosphorylated Smad1/5/8 was still able to translocate to the nucleus in the absence of TAK1, though the total levels of phosphorylated Smad1/5/8 were decreased (Supplementary Figure S3D).

Next, we examined TGFβ-induced activation of the canonical Smad and MAP kinase pathway in TAK1-deficient chondrocytes by immunoblotting for phospho-Smad2 and phospho-p38 (Figure 4F). *Tak1*^col2 cells exhibited a significant decrease in TGFβ-induced p38 phosphorylation, whereas Smad2 phosphorylation occurred normally. This is consistent with earlier studies showing a requirement for TAK1 in the MAP kinase but not the canonical Smad pathway downstream of TGFβ (Yamaguchi *et al*, 1995; Shim *et al*, 2005). Taken together, these results suggest that TAK1 is important for the activation of both the canonical Smad (Smad1/5/8) and MAP kinase pathways downstream of BMP2/7, whereas downstream of TGFβ, TAK1 is important for the activation of p38 MAP kinase but not Smad2.

TAK1 mediates phosphorylation of Smad proteins

The decreased levels of Smad1/5/8 phosphorylation in *Tak1*^col2 chondrocytes might be explained by a requirement for TAK1 in the association of the bone morphogenetic protein receptor (BMPR) complex with phosphorylated Smad1/5/8. However, immunoprecipitation analysis showed that in TAK1-deficient chondrocytes, the interaction between BMPR1A and phosphorylated Smad1/5/8 occurs normally, 5–15 min postinduction with BMP2/7 (Supplementary Figure S3E). Thus, *Tak1* deletion does not affect the stability of the interaction between the BMPR complex and phosphorylated Smad proteins.

To test whether TAK1 interacts with Smad proteins, HEK293 cells were transfected with Flag-tagged Smad proteins along with HA-tagged TAK1 (Supplementary Figure S4A). When overexpressed, Smad1, 2, 4, 5, and 8 all interact with TAK1, although the Smad4 association was weak. To test for direct interactions between TAK1 and BMP-responsive
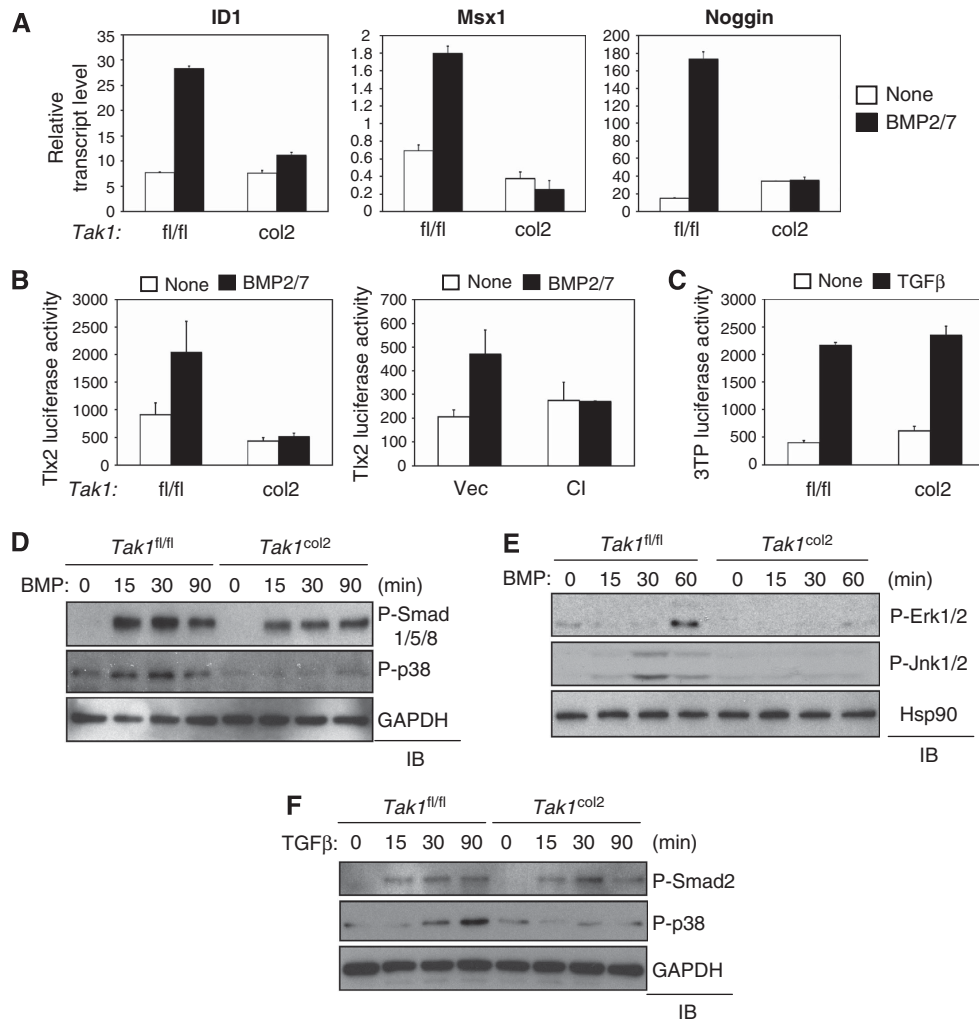
Figure 4 Reduced BMP signalling in TAK1-deficient chondrocytes. (**A**) Real time-PCR analysis for BMP-responsive gene induction in primary chondrocytes. $Tak1^{fl/fl}$ and $Tak1^{col2}$ chondrocytes were treated with or without BMP2/7 (100 ng/ml) for 6 h and total RNA was extracted for RT–PCR analysis. (**B**, **C**) Immortalized chondrocytes were transfected with either Tlx2-lux (upper panel) or 3TP-luc (lower panel) and *Renilla* luciferase vectors. Cells were serum starved for 12 h before treatment with BMP2/7 (upper panel) or TGFβ (lower panel), and then analysed for luciferase activity. Results are expressed as relative luciferase activity normalized by *Renilla* control. (**D**, **E**) Immortalized $Tak1^{fl/fl}$ and $Tak1^{col2}$ chondrocytes were serum starved for 12 h before BMP2/7 (100 ng/ml) stimulation for the indicated times, and then immunoblotted with antibodies specific to phospho-Smad1/5/8 (D), phospho-Erk1/2, or phospho-Jnk1/2 (E). Immunoblotting analysis with antibodies specific to GAPDH (D) or Hsp90 (E) was performed as a control. (**F**) Immortalized $Tak1^{fl/fl}$ and $Tak1^{col2}$ chondrocytes were serum starved for 12 h before TGFβ (2 ng/ml) stimulation for the indicated times, and then immunoblotted with antibodies specific to phospho-Smad2 and phospho-p38. Immunoblotting analysis with anti-GAPDH antibody was performed as a control.

Smad proteins, we performed a Flag pull down analysis with Flag-tagged Smad proteins and *in vitro* translated, ^{35}S-labelled TAK1 (Figure 5A, upper panel). Under these conditions, TAK1 interacted directly with Smad1, 5, and 8 and this likely occurs through the conserved MH2 domain of Smad proteins as shown in an earlier study (Hoffmann *et al*, 2005). The TAK1 domain located between aa 200 and 300 is required for binding to Smad1 (Supplementary Figure S4B). This was confirmed by a GST pull down assay with GST-Smad1 and *in vitro* translated, ^{35}S-labelled TAK1 (Figure 5A, lower panel). Importantly, analysis of endogenous TAK1 and Smad1 showed an association 5–15 min after stimulation with BMP2/7, kinetics similar to the rate of Smad1/5/8 phosphorylation indicating that TAK1 interacts with BMP-responsive Smad proteins in chondrocytes in an inducible manner (Figure 5B). In contrast, catalytically inactive TAK1 did not associate with Smad 1/5/8 although it did interact

with TAB1, a known TAK1-binding protein (Supplementary Figure S4C and D) (Komatsu *et al*, 2002; Hoffmann *et al*, 2005). These results indicate that the kinase activity of TAK1 is necessary for its interactions with Smad proteins.

As TAK1 interacts directly with Smad proteins after BMP stimulation, we tested whether TAK1 is able to induce phosphorylation of Smad proteins. *In vitro* kinase assays using HA-TAK1 immunoprecipitates from HEK293 cells transfected with HA-tagged constitutively active TAK1 (ΔN) or catalytically inactive TAK1 (CI; ΔN/K63W) (Yamaguchi *et al*, 1995) were incubated with recombinant GST, GST-Smad1, -Smad2, or -Mkk6 (Figure 5C). As expected, GST-Mkk6, a known TAK1 substrate, was phosphorylated by HA-TAK1 (ΔN), but not HA-TAK1 (CI). Notably, GST-Smad1 and -Smad2 were also both phosphorylated by HA-TAK1 (ΔN) but not HA-TAK1 (CI), indicating that TAK1 can phosphorylate Smad proteins. Given that TAK1 can bind and phos-
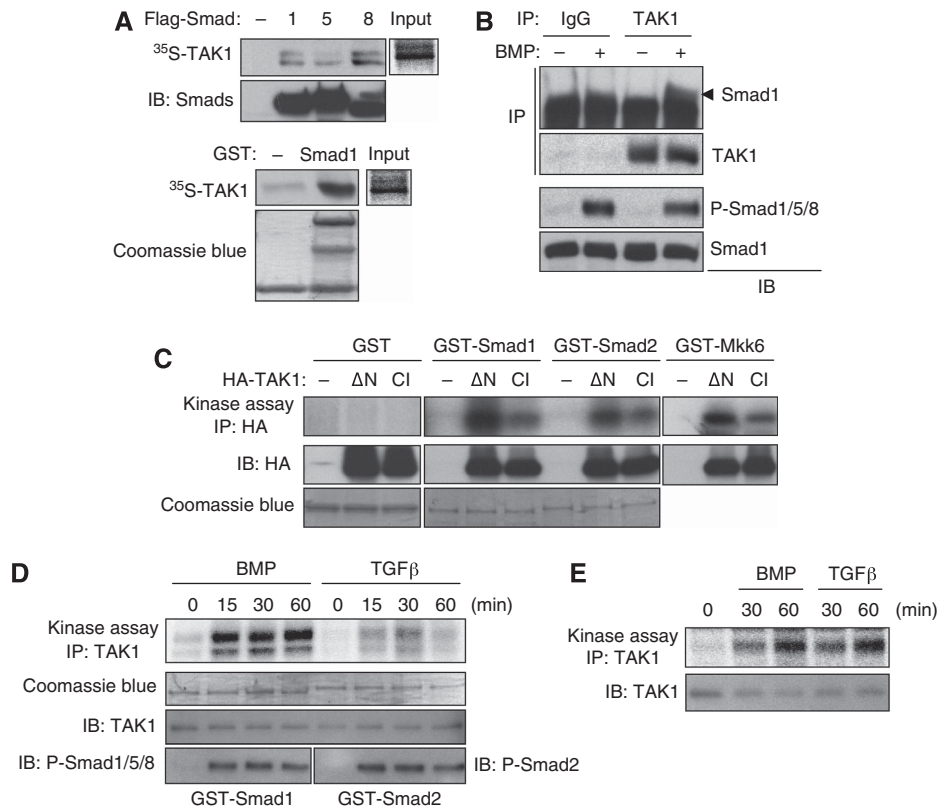
Figure 5 TAK1 is an upstream kinase of Smad proteins in BMP signalling. (**A**) Direct interaction of TAK1 with BMP-responsive Smad proteins. HEK293 cells were transfected with Flag-Smad1, 5, and 8, and lysed and immunoprecipitated with anti-Flag-conjugated beads. The interactions were tested by Flag pull down assays with Flag-Smad proteins and *in vitro* translated, ^{35}S-labelled TAK1 (upper panel). Alternatively, GST pull down analysis was performed using either GST or GST-Smad1 and *in vitro* translated, ^{35}S-labelled TAK1 (lower panel). (**B**) Endogenous interaction of TAK1 with BMP-responsive Smad proteins. Immortalized chondrocytes were serum starved before BMP2/7 (100 ng/ml) stimulation for the indicated times, and then cells were lysed, immunoprecipitated with either Rabbit IgG or anti-TAK1 antibody and protein A agarose, and immunoblotted with the indicated antibodies. (**C**) TAK1-induced phosphorylation of Smad proteins. HEK293 cells were transfected with either vector control, constitutively active HA-TAK1 (ΔN), or catalytically inactive HA-TAK1 (CI) and immunoprecipitated with anti-HA antibody and protein G agarose. The immunoprecipitates were mixed with GST, GST-Smad1, Smad2, or Mkk6, and TAK1 kinase activity was analysed by *in vitro* kinase assay. (**D, E**) TAK1 activates BMP-responsive Smad1 more efficiently than TGFβ-responsive Smad2. Immortalized wt chondrocytes were serum starved for 12 h before treatment with BMP2/7 (100 ng/ml) or TGFβ (2 ng/ml) for the indicated time and then immunoprecipitated with anti-TAK1 antibody. The immunoprecipitates were mixed with GST-Smad1 (BMP2/7), GST-Smad2 (TGFβ) (D), or GST-Mkk6 (E). TAK1 kinase activity was analysed by *in vitro* kinase assay.

phorylate both Smad1 and Smad2, it may be important for Smad phosphorylation in both BMP and TGFβ signalling pathways. To test this hypothesis, we analysed TAK1-mediated phosphorylation of Smad1 and 2 after BMP and TGFβ stimulation using *in vitro* kinase assays (Figure 5D). Surprisingly, little GST-Smad2 phosphorylation was detected in response to TGFβ, whereas GST-Smad1 was strongly phosphorylated with peak activity 15 min postinduction by BMP2/7. However, GST-Mkk6 was equivalently phosphorylated after stimulation with either TGFβ or BMP2/7, indicating that TAK1 is similarly activated downstream of TGFβ and BMP2/7 signalling (Figure 5E) (Yamaguchi *et al*, 1995). Thus, differences in the intrinsic activation status of TAK1 are unlikely to account for the selective phorphorylation of Smad1 and not Smad2 by endogenous TAK1. This may explain why the *Tak1*[col2] mice bear a much greater resemblance to mice with defects in BMP but not TGFβ signalling in chondrocytes (Yi *et al*, 2000; Yoon *et al*, 2005).

Identification of TAK1 phosphorylation sites in Smad1
Coomassie blue staining showed a slight mobility shift of the isolated Smad1 protein when co-expressed with TAK1,

implying that TAK1 induces posttranslational modification of Smad1 (Figure 6A). To identify the TAK1-mediated phosphorylation sites in Smad1, we performed mass spectrometry analysis. HEK293 cells were transfected with Flag-Smad1 together with either vector control or constitutively active TAK1 (ΔN), and immunoprecipitated using Flag-conjugated agarose. As Smad1 interacts with TAK1 through its MH2 domain, phosphopeptide analysis initially focused on this region (Figure 6A, lower panel). Mass spectrometry analysis revealed that, when co-expressed with TAK1, Smad1 is phosphorylated at C-terminal serines (S463 and S465), the same phosphorylation sites targeted by the BMP type I receptor kinase (Tables I and II) (Hoodless *et al*, 1996; Macias-Silva *et al*, 1996; Abdollah *et al*, 1997; Kretzschmar *et al*, 1997b). This is consistent with the immunoblotting analysis with anti-phospho-Smad1/5/8 (S463/S465, S426/S428) showing that Flag-Smad1 is phosphorylated at C-terminal serines in the presence of HA-TAK1 (ΔN) (Figure 6B). BMPR1 was not detectable in co-immunoprecipitations with HA-TAK1 (ΔN), making it unlikely that the S463/S465 phosphorylation observed was mediated by BMPR1 that co-purified with HA-TAK1 (Supplementary Figure S4E).
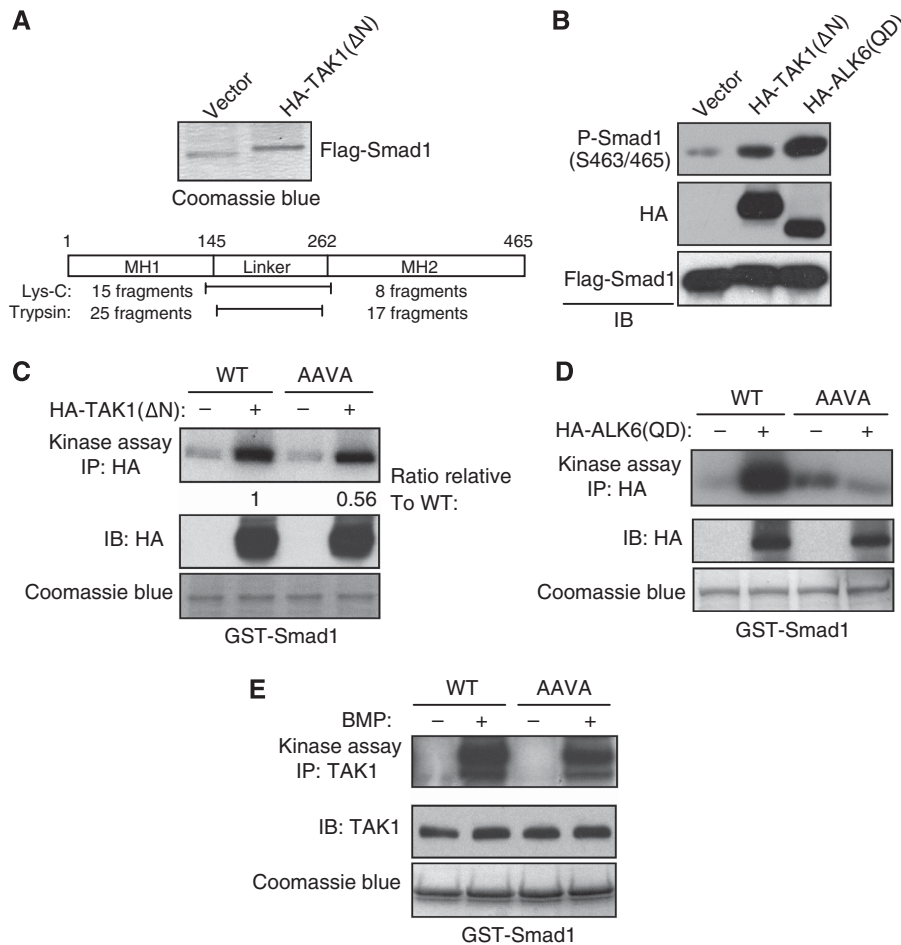
Figure 6 Identification of Smad1 phosphorylation sites by TAK1. (**A**) Phosphopeptide analysis of Smad1. HEK293 cells were transfected with Flag-Smad1 together with either vector or HA-TAK1 (ΔN). After immunoprecipitation with anti-Flag conjugated agarose, Smad1 proteins were eluted by Flag peptide, separated by SDS–PAGE, and stained with Coomassie blue (upper panel). The predicted proteolytic digestion pattern of Smad1 (lower panel). (**B**) Smad1 phosphorylation by TAK1. HEK293 cells were transfected with Flag-Smad1 together with either vector, HA-TAK1 (ΔN), or HA-BMPR1B (Q203D). Cells were lysed and immunoblotted with the indicated antibodies. (**C**) TAK1-mediated phosphorylation of Smad1 at the C-terminal serines. HEK293 cells were transfected with either vector or HA-TAK1 (ΔN), and the immunoprecipitates were mixed with wt GST-Smad1 (WT) or mutant GST-Smad1 (AAVA). TAK1 kinase activity was analysed by *in vitro* kinase assay. (**D**) BMPR1B-mediated phosphorylation of Smad1 at the C-terminal serines. HEK293 cells were transfected with either vector or HA-BMPR1B (Q203D) and the immunoprecipitates were mixed with wt GST-Smad1 (WT) or mutant GST-Smad1 (AAVA). BMPR1B kinase activity was analysed by *in vitro* kinase assay. (**E**) Immortalized chondrocytes were serum starved for 12 h before BMP2/7 (100 ng/ml) stimulation for 20 min. The TAK1 immunoprecipitates were washed under stringent conditions to minimize contamination by other endogenous proteins, mixed with GST-Smad1 (WT or AAVA), and TAK1 kinase activity was analysed by *in vitro* kinase assay.

TAK1-induced phosphorylation at C-terminal serines was weaker than phosphorylation by constitutively active BMPR1B (Q203D), implying that BMPR1B is able to phosphorylate Smad1 at C-terminal serines more efficiently than TAK1 (Figure 6B) (Hoffmann *et al*, 2005). To test the ability of TAK1 to induce Smad1 phosphorylation at C-terminal serines, we generated recombinant GST-Smad1 containing the SSVS to AAVA mutation, which is a poor substrate for the BMP type I receptor kinase (Kretzschmar *et al*, 1997b). Mutation of the S463/S465 site to AAVA led to a moderate decrease in TAK1 (ΔN)-induced phosphorylation, although it significantly decreased BMPR1B (Q203D)-induced phosphorylation (Figure 6C and D). This is consistent with immunoblotting analysis with anti-phospho-Smad1/5/8 (S463/S465, S426/S428) showing that the phosphorylation level of Smad1 at S463/S465 was moderately decreased in TAK1-deficient chondrocytes in response to BMP2/7 (Figure 4D). Similarly, the AAVA mutated Smad1 only showed a partial reduction in the level

of phosphorylation by the endogenous TAK1 complex immunoprecipitated from the *wt* chondrocyte line after BMP stimulation (Figure 6D). Thus, these results strongly suggest that TAK1 may phosphorylate Smad1 at sites in addition to S463/S465.

Requirement of TAK1 kinase activity in BMP signalling

To test the absolute requirement for TAK1 kinase activity in BMP signalling, TAK1-deficient chondrocytes were reconstituted with exogenous TAK1 using a lentiviral system (Figure 7). *Tak1*^{col2} chondrocytes were infected with either wt or CI TAK1 lentiviruses and selected in puromycin-containing medium. As expected, TAK1 (WT)-expressing cells exhibited an increase in Smad1/5/8 and p38 MAP kinase phosphorylation in response to BMP2/7. In contrast, exogenous expression of catalytically inactive TAK1 (CI) failed to restore Smad1/5/8 phosphorylation (Figure 7A).

Table I Proteolytic digestion of human Smad1 by Trypsin

Size	Vector	HA-TAK1 (ΔN)
1–15	MNVTSLFSFTSPAVK	MNVTSLFSFTSPAVK
16/17–21	R/LLGWK	R/LLGWK
22–28	QGDEEEK	QGDEEEK
29–32	WAEK	WAEK
33–39	AVDALVK	AVDALVK
40/41–42	K/LK	K/LK
43/44/45	K/K/K	K/K/K
46–53	GAMEELEK	GAMEELEK
54–69	ALSCPGQPSNCVTIPR	ALSCPGQPSNCVTIPR
70–74	SLDGR	SLDGR
75–80	LQVSHR	LQVSHR
81/82–90	K/GLPHVIYCR	K/GLPHVIYCR
91–93	VWR	VWR
94–116	WPDLQSHHELKPLECCEFPFGSK	WPDLQSHHELKPLECCEFPFGSK
117–118	QK	QK
119–128	EVCINPYHYK	EVCINPYHYK
129/130–142	R/VESPVLPPVLVPR	R/VES*PVLPPVLVPR
	R/VES*PVLPPVLVPR	
143–157	HSEYNPQHSLLAQFR	HSEYNPQHSLLAQFR
158–257	NLGQNEPHMPLNATFPDSFQQPNSHPFPHSPNSSY-PNSPGSSSSTYPHSPTSSDPGSPFQMPADTPPPAYLP-PEDPMTQDGSQPMDTNMMAPPLPSEINR	NLGQNEPHMPLNATFPDSFQQPNSHPFPHSPNSSY-PNSPGSSSSTYPHSPTSSDPGSPFQMPADTPPPAYLP-PEDPMTQDGSQPMDTNMMAPPLPSEINR
258–269	GDVQAVAYEEPK	GDVQAVAYEEPK
270–282	HWCSIVYYELNNR	HWCSIVYYELNNR
283–306	VGEAFHASSTSVLVDGFTDPSNN	VGEAFHASSTSVLVDGFTDPSNN
/307–308	K/NR	K/NR
309–319	FCLGLLSNVNR	FCLGLLSNVNR
320–327	NSTIENTR	NSTIENTR
328/329–332	R/HIGK	R/HIGK
333–358	GVHLYYVGGEVYAECLSDSSIFVQSR	GVHLYYVGGEVYAECLSDSSIFVQSR
359–373	NCNYHHGFHPTTVCK	NCNYHHGFHPTTVCK
374–381	IPSGCSLK	IPSGCSLK
382–408	IFNNQEFAQLLAQSVNHGFETVYELTK	IFNNQEFAQLLAQSVNHGFETVYELTK
409–413	MCTIR	MCTIR
414–418	MSFVK	MSFVK
419–426	GWGAEYHR	GWGAEYHR
427–449	QDVTSTPCWIEIHLHGPLQWLDK	QDVTSTPCWIEIHLHGPLQWLDK
450–465	VLTQMGSPHNPISSVS	VLTQMGSPHNPISS*VS
	VLTQMGSPHNPISS*VS	VLTQMGSPHNPISS*VS*

*Phosphorylation.

The functional response to BMP2/7 in *Tak1*col2 chondrocytes could also be reconstituted by TAK1 expression. Exogenous expression of TAK1 (WT) significantly increased ID1 expression after BMP2/7 stimulation of *Tak1*col2 chondrocytes (Miyazono and Miyazawa, 2002), whereas little induction of ID1 was detected in vector or TAK1 (CI)-expressing cells (Figure 7B). Therefore, TAK1 activates both the canonical Smad and the p38 MAP kinase pathways through its kinase activity, and this activity is important for the transcriptional response to BMP2/7.

Discussion

TAK1, a MAP3K kinase family member, was originally identified as a key mediator of the p38 MAPK kinase pathway that was activated downstream of both TGFβ and BMP4 (Yamaguchi *et al*, 1995). However, with the exception of a study in *Xenopus* demonstrating that TAK1 mediates ventral mesoderm induction and patterning downstream of BMPs, the *in vivo* role of TAK1 in BMP signalling remained unexplored (Shibuya *et al*, 1998). The involvement of BMPs in growth, patterning, and maintenance of cartilage made this organ system an attractive *in vivo* model to explore.

Early embryonic lethality in germline TAK1-deficient mice precluded genetic studies of mammalian TAK1 in skeletal biology (Shim *et al*, 2005; Jadrich *et al*, 2006). We took advantage of an earlier generated strain of mice with a conditional deletion of *Tak1* to generate mice lacking *Tak1* selectively in chondrocytes (Xie *et al*, 2006). TAK1 deficiency in chondrocytes caused a severe chondrodysplasia with runting, elbow dislocation, cartilage overgrowth, and tarsal fusion, abnormalities that are variously present in mice lacking BMPR1B, GDF5, or multiple BMP ligands (Storm *et al*, 1994; Yi *et al*, 2000; Bandyopadhyay *et al*, 2006). The observation that the *Tak1* phenotype represents a mixture of BMP-associated phenotypes indicates that TAK1 serves an essential function downstream of multiple BMP family members. Signal transduction downstream of BMPs can be considered as a dichotomy between the activation of MAP kinase pathways and the canonical Smads (Derynck and Zhang, 2003; Yoon and Lyons, 2004). Earlier, TAK1 was largely considered as a proximal activator of the MAP kinase arm of signalling, without a clear role in Smad activation (Yamaguchi *et al*, 1995). However, the reduction in both Smad and p38/Jnk/Erk MAP kinase responses in *Tak1*col2 chondrocytes indicates that TAK1 has an important but distinct function in both signalling arms downstream of BMP2/7.

Table II Proteolytic digestion of human Smad1 by Lys-C

Size	Vector	HA-TAK1 (ΔN)
1–15	MNVTSLFSFTSPAVK	MNVTSLFSFTSPAVK
16–21	RLLGWK	RLLGWK
22–28	QGDEEEK	QGDEEEK
29–32	WAEK	WAEK
33–39	AVDALVK	AVDALVK
40/41–42	K/LK	K/LK
43/44/45	K/K/K	K/K/K
46–53	GAMEELEK	GAMEELEK
54–81	ALSCPGQPSNCVTIPRSLDGRLQVSHRK	ALSCPGQPSNCVTIPRSLDGRLQVSHRK
82–116	GLPHVIYCRVWRWPDLQSHHELKPLECCEFPFGSK	GLPHVIYCRVWRWPDLQSHHELKPLECCEFPFGSK
117–118	QK	QK
119–128	EVCINPYHYK	EVCINPYHYK
129–269	RVESPVLPPVLVPRHSEYNPQHSLLAQFRNLGQNEPHM-PLNATFPDSFQQPNSHPFPHSPNSSYPNSPGSSSSTYPH-SPTSSDPGSPFQMPADTPPPAYLPPEDPMTQDGSQPMD-TNMMAPPLPSEINRGDVQAVAYEEPK	RVESPVLPPVLVPRHSEYNPQHSLLAQFRNLGQNEPHM-PLNATFPDSFQQPNSHPFPHSPNSSYPNSPGSSSSTYPH-SPTSSDPGSPFQMPADTPPPAYLPPEDPMTQDGSQPMD-TNMMAPPLPSEINRGDVQAVAYEEPK
270–306	HWCSIVYYELNNRVGEAFHASSTSVLVDGFTDPSNNK	HWCSIVYYELNNRVGEAFHASSTSVLVDGFTDPSNNK
307–332	NRFCLGLLSNVNRNSTIENTRRHIGK	NRFCLGLLSNVNRNSTIENTRRHIGK
333–373	GVHLYYVGGEVYAECLSDSSIFVQSRNCNYHHGFHPTT-VCK	GVHLYYVGGEVYAECLSDSSIFVQSRNCNYHHGFHPTT-VCK
374–381	IPSGCSLK	IPSGCSLK
382–408	IFNNQEFAQLLAQSVNHGFETVYELTK	IFNNQEFAQLLAQSVNHGFETVYELTK
409–418	MCTIRMSFVK	MCTIRMSFVK
419–449	GWGAEYHRQDVTSTPCWIEIHLHGPLQWLDK	GWGAEYHRQDVTSTPCWIEIHLHGPLQWLDK
450–465	VLTQMGSPHNPISSVS	
	VLTQMGSPHNPISS*VS	VLTQMGSPHNPISS*VS
		VLTQMGSPHNPISS*VS*

*Phosphorylation.

Comparison of the Tak1^col2 phenotype to the phenotype of mice deficient for BMP signalling

The Tak1^col2 phenotype is not identical to that of any single member of the BMP signalling pathway. The degree of runting and the delay in secondary ossification centre formation in Tak1^col2 mice resemble that seen in mice with a conditional deletion of Smad4 in chondrocytes (Zhang et al, 2005). Additionally, the magnitude of IHH downregulation in Tak1^col2 hypertrophic chondrocytes is similar to that observed in both Smad4 and BMPR1A conditional knockout mice (Yoon et al, 2006). Hence, these aspects of the Tak1^col2 phenotype may be due to dysregulation of Smad signalling downstream of BMPs. However, mice with a conditional deletion of Smad4 in chondrocytes do not display elbow dislocation or fusion of the tarsal bones. These features are reminiscent of the defects seen in BMPR1B and GDF5 knockout mice (Storm et al, 1994; Yi et al, 2000), suggesting that the GDF5 to BMPR1B signalling module that maintains the integrity of the elbow joint also uses TAK1 as a necessary signalling intermediate. The penetrance of the elbow dislocation phenotype in TAK1-deficient mice is higher (~80% by 2 weeks of age) than that observed in BMPR1B-deficient mice (23%). Combined with the earlier onset of the dislocation phenotype in TAK1-deficient mice, this finding suggests that BMPR1B may have partial functional redundancy with another receptor subunit acting upstream of TAK1. This receptor subunit is highly likely to be BMPR1A, but the severe cartilage defects in mice lacking both BMPR1A/B in cartilage make analysis of this redundancy difficult in vivo (Yoon et al, 2005).

This similarity between GDF5 and Tak1^col2 phenotypes is further supported by the finding of tarsal bone fusion (Storm et al, 1994). However, mice with a spontaneous loss-of-function mutation in GDF5 show only a slight shortening of

the long bones, implicating other BMP family members upstream of TAK1. Additionally, although GDF5 mutant mice do have fusion of the tarsal bones, they do not display the marked medial deviation of the hindlimb phalanges seen in Tak1^col2 mice, indicating that this deviation is not simply secondary to ankle bone malformation. As these aspects of the phenotype (elbow dislocation, tarsal fusion) are present in GDF5 and BMPR1B but not Smad4-defivent mice, they may be MAP kinase dependent. However, the role of the MAP kinase pathway in postnatal cartilage growth and development has not been explored as thoroughly in vivo as the role of the Smad pathway, making it difficult to examine the contribution of MAP kinase signalling to the Tak1^col2 phenotype.

TAK1 mediates phosphorylation of Smad proteins downstream of BMPs but not TGFβ

The TAK1 phenotype is notable for the absence of specific features of mice genetically unable to respond to TGFβ in chondrocytes. In particular, mice with a deletion of TGFβR2 in chondrocytes display abnormalities in the axial skeleton, including bifurcation of the xiphoid process, abnormal morphogenesis of the C1, C2 vertebrae, and malformation of the vertebral transverse processes, which are not present in Tak1^col2 mice (Serra et al, 1997; Baffi et al, 2004). In our study, analysis of primary and transformed chondrocytes revealed that TAK1 is able to phosphorylate Smad proteins in response to BMP2/7 but not TGFβ. However, Smad1 (a BMP-responsive Smad) and Smad2 (a TGFβ-responsive Smad) can both be phosphorylated by overexpressed, constitutively active TAK1, indicating that TAK1 has an equivalent intrinsic ability to phosphorylate both substrates. Additionally, phosphorylation of MKK6 by TAK1 is similar after BMP2/7 and TGFβ stimulation, indicating that the
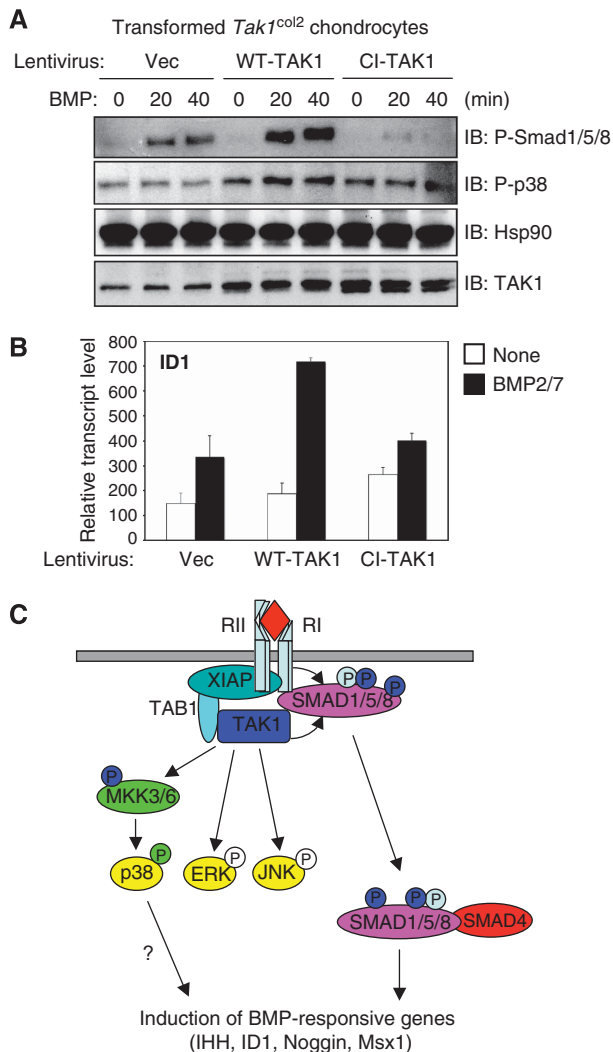
Figure 7 TAK1 kinase activity is important for BMP signalling. (**A**, **B**) Immortalized chondrocytes were infected either by vector control, TAK1 (WT), or TAK1 (CI) lentiviruses and selected in puromycin-containing medium. (A) Cells were serum starved for 12 h before BMP2/7 (100 ng/ml) stimulation for the indicated time and immunoblotted with antibodies specific to phospho-Smad1/5/8 and phospho-p38. Immunoblotting with anti-Hsp90 and -TAK1 antibodies were performed for protein loading control and TAK1 expression, respectively. (B) Alternatively, cells were unstimulated or stimulated with BMP2/7 for 6 h and total RNA was extracted for RT–PCR analysis. (**C**) Schematic model of TAK1 function in BMP signalling pathways.

activation of TAK1 kinase is similar downstream of each ligand (Yamaguchi *et al*, 1995). Recently, it has been reported that the activated TGFβ receptor 1 recruits TRAF6 to the receptor complex and subsequently induces ubiquitination of TRAF6 and promotes TRAF6 interaction with TAK1, thereby resulting in activation of p38/JNK MAP kinases (Sorrentino *et al*, 2008; Yamashita *et al*, 2008). However, the mechanism of TAK1-mediated p38 MAP kinase activation downstream of BMP signalling has not been explored. Given these observations, the most likely explanation for the selective involvement of TAK1 in Smad phosphorylation downstream of BMP but not TGFβ stimulation is that another component of the TGFβ receptor complex acts to block TAK1 access to Smad2. For such a mechanism to be effective, the active fraction of

TAK1 must be sequestered at the TGFβ receptor complex. Likewise, either the BMP receptor complex is permissive for TAK1 and Smad1/5/8 interactions or TAK1 is released from the receptor complex to phosphorylate Smad1/5/8 in the cytosol.

TAK1-inducible phosphorylation of Smad1 at multiple sites

The finding that phosphorylation levels of Smad1/5/8 at C-terminal serines were reduced both *in vivo* and *in vitro* in response to BMP stimulation suggested an unexpected role for TAK1 in regulating the activity of BMP-responsive Smads. As the immunoprecipitated TAK1 protein was able to phosphorylate Smad1 protein in *in vitro* kinase assays, we undertook a systematic analysis of Smad1 phosphorylation using a mass spectrometry approach (Figure 6A; Tables I and II). This analysis showed that phosphorylation of Smad1 at the C-terminal serines S463/S465 was increased by co-expression of constitutively active TAK1. Mutation of this site confirmed this finding, showing an approximately 40% reduction in TAK1-mediated phosphorylation. Additionally, our *in vivo* and *in vitro* data show that S463/S465 phosphorylation was moderately decreased in both hypertrophic chondrocytes and the *Tak1*col2 chondrocyte line after BMP2/7 stimulation (Figures 3A, B and 4D). As S463/S465 phosphorylation is critical for Smad1 activity (Kretzschmar *et al*, 1997b), a reduction in S463/S465 phosphorylation would explain the reduction in BMP signalling observed both *in vivo* and *in vitro* in TAK1-deficient chondrocytes. This implies that TAK1 may have a function in amplification of the signal from the BMP receptor by increasing phosphorylation at the same S463/S465 site targeted by the BMPR1 kinase activity.

The partial reduction in Smad1 phosphorylation observed in S463/S465 mutated Smad1 (AAVA Smad1) indicates that additional sites are phosphorylated by TAK1 (Figure 6C and E). Further, the absence of detectable phosphorylation sites in the MH1 and MH2 domain by the phosphopeptide analysis suggests that these additional sites might lie inside the linker region. Unfortunately, the lack of Trypsin and Lys-C cleavable sites precluded finding phosphorylation site in this region. It has been reported that the Smad1 linker region contains four MAPK phosphorylation sites and two Gsk3β sites and MAPK and Gsk3β phosphorylation of the linker region restricts Smad1 activity by recruiting the ubiquitin ligase Smurf1, leading to degradation of Smad1 (Kretzschmar *et al*, 1997a; Fuentealba *et al*, 2007; Sapkota *et al*, 2007). As phosphorylation of these sites is important for the regulation of FGF/BMP pathway crosstalk, it will be interesting to test the possibility that TAK1 is involved in the regulation of BMP signalling by FGF through its phosphorylation of those linker phosphorylation sites. However, the critical role of TAK1 in BMP signalling precludes an analysis of this crosstalk until a component of the MAPK cascade downstream of TAK1-mediated BMP signalling is identified.

A model of BMP receptor complex assembly

Analysis of the associations among TAK1, BMPR1A, and the adaptor proteins XIAP and TAB1 suggests a mechanism for TAK1 recruitment to the BMP receptor complex. In BMP signalling pathways, X-linked inhibitor of apoptosis protein (XIAP) functions as an adapter protein that connects the BMPR complex with the TAB1–TAK1 complex through its

association with TAB1 and BMPR1A (Shibuya et al, 1998; Yamaguchi et al, 1999). Our in vitro experiments demonstrate that BMPR1A binds to XIAP, XIAP in turn mediates the interaction between BMPR1A and TAB1, and TAB1 mediates the interaction between XIAP and TAK1 (Supplementary Figure S5A–C). As the interaction of BMPR1A with XIAP occurs normally in TAK1-deficient chondrocytes, TAK1 functions downstream of the BMPR–XIAP complex (Supplementary Figure S5D).

Hence, we propose a model wherein BMPR1A is connected to the TAK1 complex (TAK1–TAB1) through XIAP, and TAK1 mediates canonical Smad and p38 MAP kinase activation downstream of BMP signalling (Figure 7C). On BMP stimulation, the activated BMPRI recruits Smad 1/5/8 directly, and the TAK1 complex (TAK1–TAB1) is recruited to the receptor by the adaptor XIAP. R-Smads can be phosphoryated by the type I BMPR and TAK1 at either S463/465 (Smad1/5) or S426/428 (Smad8). Activated R-Smads, in turn, bind to Smad4, translocate into the nucleus, and mediate BMP-responsive gene expression (i.e. IHH, ID1, Noggin, and Msx1). Alternatively, the TAK1 complex can activate the MKK3/6-p38 MAP kinase pathway.

Our results do not exclude the possibility that TAK1 may participate in the regulation of other BMP signalling intermediates and other signalling pathways. Indeed, in TAK1-deficient chondrocytes, a decreased phosphorylation of p38 MAP kinase was detected in response to TGFβ, and phosphorylation of JNK and ERK MAP kinases and IκBα was also decreased after BMP stimulation (Figure 4D and F and data not shown).

Materials and methods

Cells, plasmids, and antibodies

HEK 293 cells (human kidney embryonic cells) were purchased from ATCC and cultured in DMEM medium (Cellgro) containing 10% FBS, 2 mM L-glutamine and 1% penicillin/streptomycin. Primary and immortalized chondrocytes were cultured in DMEM-F12 medium (Cellgro) containing 2% FBS, 2 mM L-glutamine, 1% penicillin/streptomycin, 1% non-essential amino acids, Na-Selenate and transferrin. Plasmids for HA-ALK3, Myc-XIAP and HA-TAK1 (WT, ΔN, and ΔN/K63W), SV40 large T Ag, Myc-tagged TAK1 mutants, and GST-Smad1, 2, 3, and 4 were the gifts of Drs Hiroshi Shibuya, Kunihiro Matsumoto, Jun Ninomiya-Tsuji, Nobuyuki Tanaka, Xia-fan Wang, Ki-young Lee, and Zhijie Chang, respectively. Plasmid for LPCX-BMPR1B (Q203D) was purchased from Addgene. GST-Smad1 (AAVA) and TAK1 (WT and ΔN/K63W) cDNAs were PCR amplified and cloned into pGEX vector (Amersham Pharmacia) and pHASE/PGK-PURO lentiviral vector, respectively. Antibodies used were anti-TAK1 (Millipore); anti-HA, anti-c-Myc, and anti-BMPR-1A (Santa Cruz); anti-Smad2, anti-phospho-Smad1/5/8, anti-phospho-Smad2 (S465/467), and anti-phospho-p38 (Cell Signaling); anti-Smad1 (Invitrogen); anti-Flag (M2, Sigma); anti-Smad4 (Abcam); anti-XIAP (Stressgen); and anti-GAPDH (Affinity Bioreagents). Cells were treated with rhBMP2/7 and mTGFβ (R&D Systems) as indicated. To minimize interference of XIAP detection by the heavy and light chains of the immunoprecipitating BMPR1A antibody, mouse Trueblot ULTRA kit (eBioscience) was used for interaction analysis of BMPR1A with XIAP (Supplementary Figure S5E).

Generation of cartilage-specific TAK1-deficient mice

Tak1$^{fl/fl}$ mice were intercrossed with the earlier described Col2-cre deleter strain to generate Tak1$^{fl/fl}$·Col2-cre mice (Ovchinnikov et al, 2000). As Tak1$^{fl/fl}$·Col2-cre mice do not survive beyond 3 weeks of age, the line was maintained as an intercross of Tak1$^{fl/+}$·Col2-cre and Tak1$^{fl/fl}$ mice. Animals were maintained in accordance with the NIH Guide for the Care and Use of Laboratory Animals and were

handled according to protocols approved by the institution's subcommittee on animal care (IACUC).

Generation of mouse chondrocytes

Chondroepiphyses were dissected from the long bones of day 1 newborn pups from the intercross of Tak1$^{fl/+}$·Col2-cre and Tak1$^{fl/fl}$ mice. They were washed with PBS and incubated with 2 mg/ml collagenase P (Roche) for 2–4 h at 37°C. The cell suspension was plated in six-well plates containing DMEM-F12 supplemented with 2% FBS (Gosset et al, 2008). Tak1$^{fl/fl}$·Col2-cre chondrocytes were identified by immunoblotting with TAK1 antibody and PCR genotyping using tail DNA. To immortalize primary chondrocytes, cells were stably transfected with linearized SV40 Large T antigen plasmid (Kobayashi et al, 2005; Shim et al, 2005) using Effectene trasnfection reagent (Qiagen).

Skeletal preparation and histology

The mineralization pattern of the skeleton was analysed at 20 days after birth using the method of McLeod (McLeod, 1980). Briefly, mice were killed by CO$_2$ narcosis, skinned, eviscerated, and fixed in 95% ethanol. Then skeletons were stained by Alizarin red S/Alcian blue and sequentially cleared in 1% potassium hydroxide. For histological analyses, paraffin sections of bones were produced from E18.5, p0, and p20 mice. Limb tissues were dissected and fixed in 4% paraformaldehyde (PFA) in PBS. They were then decalcified by daily changes of 15% tetrasodium EDTA until soft and pliable. Tissues were dehydrated by passage through an ethanol series, cleared twice in xylene, embedded in paraffin, and sectioned. For morphological analyses, tissue sections were stained with haematoxylin and eosin.

In situ hybridization

For in situ hybridization, probe plasmids of Collagen X, IHH, and ID1 were kindly provided by Drs Bjorn Olsen, Beate Lanske, and Kuni Tsuji, respectively. DIG labelled probes were prepared using the DIG labelling kit (Roche) as per the manufacturer's instructions. Briefly, probes were purified by washing over a Ultrafree-MC filter column (Millipore). Tissue sections were prewarmed at 55°C and deparaffinized and rehydrated by passage through xylene and 100, 95, and 70% ethanol. Endogenous peroxidase activity was quenched by 15 min incubation in 3% hydrogen peroxide. Samples were treated with 10 μg/ml proteinase K for 15 min, 4% PFA for 5 min, and 0.25% acetic acid for 15 min before being dehydrated by passage through increasing concentrations of ethanol. Probe was added to the hybridization solution (50% formamide, 10 mM Tris–HCl pH 7.5, 200 μg/ml tRNA, 1 × Denhardt's, 10% Dextran sulphate, 600 mM NaCl, 0.25% SDS, 1 mM EDTA) and the solution prewarmed to 85°C before incubation with the tissue sections overnight. After incubation, sections were washed with standard sodium citrate buffer and treated with 10 μg/ml RNaseA in TNE buffer (10 mM Tris–HCl, 100 mM NaCl, 1 mM EDTA). DIG-labelled probe was then detected by immunostaining with anti-DIG-POD and streptadvidin-horseradish peroxidase.

Immunohistochemistry

For IHC, paraffin tissue sections were de-waxed and endogenous peroxidase quenched as in preparation for in situ hybridization. For anti-TAK1 staining, sections were then incubated with hyaluronidase. For anti-phospho-Smad1/5/8 staining, sections were heated in a pressure cooker. Sections were blocked with 3% goat serum, 1% BSA, 0.1% Triton X 100 in PBS for 1 h at room temperature and incubated with antibodies specific for TAK1 or phospho-Smad1/5/8 at 4°C overnight. Sections were then treated with TSA-biotin (Perkin Elmer) and streptavidin-HRP as per manufacturer's instructions, and HRP visualized with DAB (2,2′-diaminobenzidine tetrahydrochloride).

Phosphopeptide analysis

HEK293 cells grown on three 10 cm petri dishes were transiently transfected using Effectene transfection reagent (Qiagen) with Flag-Smad1 together with either vector or HA-TAK1 (ΔN). Flag-Smad1 protein was immunoprecipitated with anti-Flag conjugated agarose overnight at 4°C, eluted by Flag peptide, separated by SDS–PAGE, and stained with coomassie blue. Gel band containing Flag-Smad1 was excised and subjected to in-gel reduction and alkylation followed by Lys-C or trypsin digestion. Digested peptides were extracted from the gel and analysed by liquid chromatography

MS/MS (LC-MS/MS). Peptides were separated across a 37-min gradient ranging from 4 to 27% (v/v) acetonitrile in 0.1% (v/v) formic acid in a microcapillary ($125\,\mu m \times 18\,cm$) column packed with C_{18} reverse-phase material (Magic C18AQ, $5\,\mu m$ particles, $200\,\text{Å}$ pore size, Michrom Bioresources) and on-line analysed on The LTQ Orbitrap XL$^{\text{TM}}$ hybrid FTMS (Thermo Fisher Scientific). For each cycle, one full MS scan acquired on the Orbitrap at high mass resolution was followed by 10 MS/MS spectra on the linear ion trap XL from the 10 most abundant ions. MS/MS spectra were searched using the Sequest algorithm against Smad1 protein with dynamic modification of methionine oxidation and serine, threonine and tyrosine phosphorylation. All peptide matches were filtered based on mass deviation, tryptic state, XCorr, and dCn and confirmed by manual validation.

Luciferase reporter assay

Immortalized chondrocytes grown on 12-well plates were transiently transfected using Effectene transfection reagent (Qiagen) with the BMP (Tlx2-lux) or TGFβ-dependent reporter construct (3TP-luc) together with the Renilla luciferase vector (Promega). Total DNA concentration in each experiment was maintained by adding the appropriate control vector to the DNA mixture. At 24 h after transfection, cells were serum starved for 12 h before treatment with BMP2/7 or TGFβ. After 24 h, cells were lysed and luciferase activity was measured using the dual luciferase assay kit (Promega).

In vitro kinase assay

For in vitro kinase assays, immortalized chondrocytes grown on 10 cm petri dishes were serum starved for 12 h before treatment with either BMP2/7 (100 ng/ml) or TGFβ (2 ng/ml) and then lysed in TNT lysis buffer (1% triton X-100, 50 mM Tris, pH 7.5, 200 mM NaCl, protease inhibitors). Alternatively, HEK293 cells were transiently transfected with vector, HA-tagged TAK1 (ΔN or CI).

Protein levels in each lysate were determined using a Bio-Rad protein assay kit (Bio-Rad) and then normalized among the samples. Protein from lysates was immunoprecipitated using either anti-TAK1 antibody or Rabbit IgG and protein A-sepharose or anti-HA conjugated agarose overnight at $4^{\circ}C$ and precipitates were incubated for 15 min at $30^{\circ}C$ in kinase buffer (20 mM HEPES, pH 7.5, 20 mM $MgCl_2$, 1 mM EDTA, 2 mM NaF, 2 mM-glycerophosphate, 1 mM DTT, $10\,\mu M$ ATP) containing appropriate GST-fused Smad proteins and $10\,\mu Ci$ of [γ32P]ATP (PerkinElmer). The substrates were then precipitated using glutathione-agarose (Novagen), resolved by SDS–PAGE and phosphorylated proteins were visualized by autoradiography.

Supplementary data

Supplementary data are available at The EMBO Journal Online (http://www.embojournal.org).

Conflict of interest

The authors declare that they have no conflict of interest.

References

Abdollah S, Macias-Silva M, Tsukazaki T, Hayashi H, Attisano L, Wrana JL (1997) TbetaRI phosphorylation of Smad2 on Ser465 and Ser467 is required for Smad2-Smad4 complex formation and signaling. J Biol Chem 272: 27678–27685

Baffi MO, Slattery E, Sohn P, Moses HL, Chytil A, Serra R (2004) Conditional deletion of the TGF-beta type II receptor in Col2a expressing cells results in defects in the axial skeleton without alterations in chondrocyte differentiation or embryonic development of long bones. Dev Biol 276: 124–142

Bandyopadhyay A, Tsuji K, Cox K, Harfe BD, Rosen V, Tabin CJ (2006) Genetic analysis of the roles of BMP2, BMP4, and BMP7 in limb patterning and skeletogenesis. PLoS Genet 2: e216

Binato R, Alvarez Martinez CE, Pizzatti L, Robert B, Abdelhay E (2006) SMAD 8 binding to mice Msx1 basal promoter is required for transcriptional activation. Biochem J 393 (Pt 1): 141–150

Chang H, Huylebroeck D, Verschueren K, Guo Q, Matzuk MM, Zwijsen A (1999) Smad5 knockout mice die at mid-gestation due to multiple embryonic and extraembryonic defects. Development 126: 1631–1642

Derynck R, Zhang YE (2003) Smad-dependent and Smad-independent pathways in TGF-beta family signalling. Nature 425: 577–584

Fuentealba LC, Eivers E, Ikeda A, Hurtado C, Kuroda H, Pera EM, De Robertis EM (2007) Integrating patterning signals: Wnt/GSK3 regulates the duration of the BMP/Smad1 signal. Cell 131: 980–993

Gosset M, Berenbaum F, Thirion S, Jacques C (2008) Primary culture and phenotyping of murine chondrocytes. Nat Protoc 3: 1253–1260

Grimsrud CD, Romano PR, D'Souza M, Puzas JE, Schwarz EM, Reynolds PR, Roiser RN, O'Keefe RJ (2001) BMP signaling stimulates chondrocyte maturation and the expression of Indian hedgehog. J Orthop Res 19: 18–25

Hoffmann A, Preobrazhenska O, Wodarczyk C, Medler Y, Winkel A, Shahab S, Huylebroeck D, Gross G, Verschueren K (2005) Transforming growth factor-beta-activated kinase-1 (TAK1), a MAP3K, interacts with Smad proteins and interferes with osteo-

genesis in murine mesenchymal progenitors. J Biol Chem 280: 27271–27283

Hoodless PA, Haerry T, Abdollah S, Stapleton M, O'Connor MB, Attisano L, Wrana JL (1996) MADR1, a MAD-related protein that functions in BMP2 signaling pathways. Cell 85: 489–500

Jadrich JL, O'Connor MB, Coucouvanis E (2006) The TGF beta activated kinase TAK1 regulates vascular development in vivo. Development 133: 1529–1541

Kameda T, Koike C, Saitoh K, Kuroiwa A, Iba H (1999) Developmental patterning in chondrocytic cultures by morphogenic gradients: BMP induces expression of indian hedgehog and noggin. Genes Cells 4: 175–184

Kobayashi H, Tanaka N, Asao H, Miura S, Kyuuma M, Semura K, Ishii N, Sugamura K (2005) Hrs, a mammalian master molecule in vesicular transport and protein sorting, suppresses the degradation of ESCRT proteins signal transducing adaptor molecule 1 and 2. J Biol Chem 280: 10468–10477

Komatsu Y, Shibuya H, Takeda N, Ninomiya-Tsuji J, Yasui T, Miyado K, Sekimoto T, Ueno N, Matsumoto K, Yamada G (2002) Targeted disruption of the Tab1 gene causes embryonic lethality and defects in cardiovascular and lung morphogenesis. Mech Dev 119: 239–249

Kretzschmar M, Doody J, Massague J (1997a) Opposing BMP and EGF signalling pathways converge on the TGF-beta family mediator Smad1. Nature 389: 618–622

Kretzschmar M, Liu F, Hata A, Doody J, Massague J (1997b) The TGF-beta family mediator Smad1 is phosphorylated directly and activated functionally by the BMP receptor kinase. Genes Dev 11: 984–995

Kronenberg HM (2003) Developmental regulation of the growth plate. Nature 423: 332–336

Liu HH, Xie M, Schneider MD, Chen ZJ (2006) Essential role of TAK1 in thymocyte development and activation. Proc Natl Acad Sci USA 103: 11677–11682

Macias-Silva M, Abdollah S, Hoodless PA, Pirone R, Attisano L, Wrana JL (1996) MADR2 is a substrate of the TGFbeta receptor and its phosphorylation is required for nuclear accumulation and signaling. Cell 87: 1215–1224

Massague J (1998) TGF-beta signal transduction. *Ann Rev Biochem* **67:** 753–791

McLeod MJ (1980) Differential staining of cartilage and bone in whole mouse fetuses by alcian blue and alizarin red S. *Teratology* **22:** 299–301

Miyazono K, Miyazawa K (2002) Id: a target of BMP signaling. *Sci STKE* **2002:** PE40

Omori E, Matsumoto K, Sanjo H, Sato S, Akira S, Smart RC, Ninomiya-Tsuji J (2006) TAK1 is a master regulator of epidermal homeostasis involving skin inflammation and apoptosis. *J Biol Chem* **281:** 19610–19617

Ovchinnikov DA, Deng JM, Ogunrinu G, Behringer RR (2000) Col2a1-directed expression of Cre recombinase in differentiating chondrocytes in transgenic mice. *Genesis* **26:** 145–146

Sapkota G, Alarcon C, Spagnoli FM, Brivanlou AH, Massague J (2007) Balancing BMP signaling through integrated inputs into the Smad1 linker. *Mol Cell* **25:** 441–454

Sato S, Sanjo H, Takeda K, Ninomiya-Tsuji J, Yamamoto M, Kawai T, Matsumoto K, Takeuchi O, Akira S (2005) Essential function for the kinase TAK1 in innate and adaptive immune responses. *Nat Immunol* **6:** 1087–1095

Sato S, Sanjo H, Tsujimura T, Ninomiya-Tsuji J, Yamamoto M, Kawai T, Takeuchi O, Akira S (2006) TAK1 is indispensable for development of T cells and prevention of colitis by the generation of regulatory T cells. *Int Immunol* **18:** 1405–1411

Sayama K, Hanakawa Y, Nagai H, Shirakata Y, Dai X, Hirakawa S, Tokumaru S, Tohyama M, Yang L, Sato S, Shizuo A, Hashimoto K (2006) Transforming growth factor-beta-activated kinase 1 is essential for differentiation and the prevention of apoptosis in epidermis. *J Biol Chem* **281:** 22013–22020

Serra R, Johnson M, Filvaroff EH, LaBorde J, Sheehan DM, Derynck R, Moses HL (1997) Expression of a truncated, kinase-defective TGF-beta type II receptor in mouse skeletal tissue promotes terminal chondrocyte differentiation and osteoarthritis. *J Cell Biol* **139:** 541–552

Shibuya H, Iwata H, Masuyama N, Gotoh Y, Yamaguchi K, Irie K, Matsumoto K, Nishida E, Ueno N (1998) Role of TAK1 and TAB1 in BMP signaling in early Xenopus development. *EMBO J* **17:** 1019–1028

Shim JH, Xiao C, Paschal AE, Bailey ST, Rao P, Hayden MS, Lee KY, Bussey C, Steckel M, Tanaka N, Yamada G, Akira S, Matsumoto K, Ghosh S (2005) TAK1, but not TAB1 or TAB2, plays an essential role in multiple signaling pathways *in vivo*. *Genes Dev* **19:** 2668–2681

Sorrentino A, Thakur N, Grimsby S, Marcusson A, von Bulow V, Schuster N, Zhang S, Heldin CH, Landstrom M (2008) The type I TGF-beta receptor engages TRAF6 to activate TAK1 in a receptor kinase-independent manner. *Nat Cell Biol* **10:** 1199–1207

Storm EE, Huynh TV, Copeland NG, Jenkins NA, Kingsley DM, Lee SJ (1994) Limb alterations in brachypodism mice due to mutations in a new member of the TGF beta-superfamily. *Nature* **368:** 639–643

Tang M, Wei X, Guo Y, Breslin P, Zhang S, Wei W, Xia Z, Diaz M, Akira S, Zhang J (2008) TAK1 is required for the survival of hematopoietic cells and hepatocytes in mice. *J Exp Med* **205:** 1611–1619

Wan M, Cao X (2005) BMP signaling in skeletal development. *Biochem Biophys Res Commun* **328:** 651–657

Wan YY, Chi H, Xie M, Schneider MD, Flavell RA (2006) The kinase TAK1 integrates antigen and cytokine receptor signaling for T cell development, survival and function. *Nat Immunol* **7:** 851–858

Winnier G, Blessing M, Labosky PA, Hogan BL (1995) Bone morphogenetic protein-4 is required for mesoderm formation and patterning in the mouse. *Genes Dev* **9:** 2105–2116

Wozney JM, Rosen V, Celeste AJ, Mitsock LM, Whitters MJ, Kriz RW, Hewick RM, Wang EA (1988) Novel regulators of bone formation: molecular clones and activities. *Science* **242:** 1528–1534

Xie M, Zhang D, Dyck JR, Li Y, Zhang H, Morishima M, Mann DL, Taffet GE, Baldini A, Khoury DS, Schneider MD (2006) A pivotal role for endogenous TGF-beta-activated kinase-1 in the LKB1/AMP-activated protein kinase energy-sensor pathway. *Proc Natl Acad Sci USA* **103:** 17378–17383

Yamaguchi K, Nagai S, Ninomiya-Tsuji J, Nishita M, Tamai K, Irie K, Ueno N, Nishida E, Shibuya H, Matsumoto K (1999) XIAP, a cellular member of the inhibitor of apoptosis protein family, links the receptors to TAB1-TAK1 in the BMP signaling pathway. *EMBO J* **18:** 179–187

Yamaguchi K, Shirakabe K, Shibuya H, Irie K, Oishi I, Ueno N, Taniguchi T, Nishida E, Matsumoto K (1995) Identification of a member of the MAPKKK family as a potential mediator of TGF-beta signal transduction. *Science* **270:** 2008–2011

Yamashita M, Fatyol K, Jin C, Wang X, Liu Z, Zhang YE (2008) TRAF6 mediates Smad-independent activation of JNK and p38 by TGF-beta. *Mol Cell* **31:** 918–924

Yi SE, Daluiski A, Pederson R, Rosen V, Lyons KM (2000) The type I BMP receptor BMPRIB is required for chondrogenesis in the mouse limb. *Development* **127:** 621–630

Yoon BS, Lyons KM (2004) Multiple functions of BMPs in chondrogenesis. *J Cell Biochem* **93:** 93–103

Yoon BS, Ovchinnikov DA, Yoshii I, Mishina Y, Behringer RR, Lyons KM (2005) Bmpr1a and Bmpr1b have overlapping functions and are essential for chondrogenesis *in vivo*. *Proc Natl Acad Sci USA* **102:** 5062–5067

Yoon BS, Pogue R, Ovchinnikov DA, Yoshii I, Mishina Y, Behringer RR, Lyons KM (2006) BMPs regulate multiple aspects of growth-plate chondrogenesis through opposing actions on FGF pathways. *Development* **133:** 4667–4678

Zhang J, Tan X, Li W, Wang Y, Wang J, Cheng X, Yang X (2005) Smad4 is required for the normal organization of the cartilage growth plate. *Dev Biol* **284:** 311–322